

Heavy Quark Symmetry in Nonleptonic B-Decays to Excited Charmed Mesons

Sonny Mantry¹

¹*Center for Theoretical Physics, Massachusetts Institute for Technology,
Cambridge, MA 02139**

Abstract

We show in a model independent way the equality of the branching fractions and strong phases for $\bar{B} \rightarrow D_1 M$ and $\bar{B} \rightarrow D_2^* M$ at leading order in Λ_{QCD}/Q and $\alpha_s(Q)$ where $Q = \{m_b, m_c, E_M\}$ and M is a light meson. These results apply in the color allowed and color suppressed channels and follow from a factorization theorem in SCET combined with heavy quark symmetry. The expected heavy quark symmetry suppression of leading order contributions in the color allowed sector based on analysis of semileptonic decays, is shown to disappear at maximum recoil. Subleading corrections are suppressed by at least one power of Λ_{QCD}/Q and this is explicitly verified for subleading semileptonic form factors at maximum recoil.

* Electronic address: mantry@mit.edu

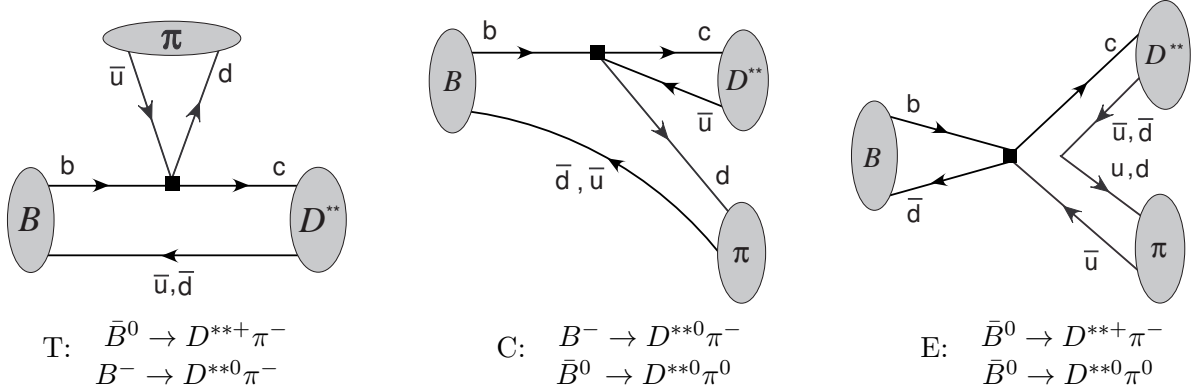


FIG. 1: Topologies contributing to $\bar{B} \rightarrow D^{**} M$ decays where M is a light meson. The diagrams are shown for the simplest case of the $D^{**}\pi$ final state.

I. INTRODUCTION

Two-body non-leptonic B -decays have generated considerable theoretical interest [1, 2, 3, 4, 5, 6, 7, 8, 9, 10, 11, 12, 13, 14, 15, 16] in recent years. Most recently, Soft Collinear Effective Theory(SCET) [17, 18] has been used with remarkable success in understanding such decays. Using SCET, B -decays of the type $\bar{B} \rightarrow D^{(*)} M$ [19] where $M = \pi, \rho, K, K^*$ have been studied in quite some detail. In this paper, we investigate such decays when the final state charmed meson is in an orbitally excited state such as the D_1 and D_2^* (see Table I) collectively referred to as D^{**} .

$\bar{B} \rightarrow D^{**} K$ decays have been recently proposed [20] as candidates for a theoretically clean extraction of the CKM angle γ making such decays all the more interesting to study. These decays also raise interesting questions regarding the power counting scheme used to make quantitative phenomenological predictions. Based on analysis of semileptonic decays [21] near zero recoil, the leading order contributions are expected to be suppressed due to heavy quark symmetry constraints. This suggests that subleading contributions could have a significant effect on leading order predictions in $\bar{B} \rightarrow D^{**} M$ type processes. We will address these issues on power counting and provide a resolution. On another note, the $\bar{B}^0 \rightarrow D^{(*)0} \rho^0$ rates are more difficult to extract cleanly from experimental data due to background contributions from intermediate D^{**} states. In particular, in the D^{*0} channel only an upper bound on the branching fraction has been measured [22] and the errors in the D^0 channel are still fairly large [23]. This has made it difficult to test the SCET prediction [19] relating the D and D^* amplitudes. With the ρ^0 meson primarily decaying to $\pi^+ \pi^-$ and the excited D^{**+} mesons decaying to $D^{(*)0} \pi^+$ the same final state is observed for $\bar{B}^0 \rightarrow D^{**+} \pi^-$ and $\bar{B}^0 \rightarrow D^{(*)0} \rho^0$. Thus, a precise extraction of the $\bar{B}^0 \rightarrow D^{(*)0} \rho^0$ rates requires us to better understand B decays to excited charmed mesons.

The $\bar{B} \rightarrow (D^{(*)}, D^{**}) M$ decays proceed via three possible topologies shown in Fig. 1 for the case of a $D^{**}\pi$ final state. In the T (tree) topology the light meson is produced directly at the weak vertex. In the C (color suppressed) and E (W-exchange or weak annihilation) topologies, a spectator quark ends up in the final state light meson. The C and E topologies are suppressed in the large N_c limit. The $\bar{B}^0 \rightarrow D^{(*)0} M^0$ type decays that proceed exclusively through these C and E topologies will be generically referred to as the color suppressed modes. Other decay channels that are dominated by the T topology will be referred to as the color allowed modes.

Mesons	$s_l^{\pi_l}$	J^P	$\bar{m}(\text{GeV})$
(D, D^*)	$\frac{1}{2}^-$	$(0^-, 1^-)$	1.971
(D_0^*, D_1^*)	$\frac{1}{2}^+$	$(0^+, 1^+)$	2.40
(D_1, D_2^*)	$\frac{3}{2}^+$	$(1^+, 2^+)$	2.445

TABLE I: The HQS doublets are labeled by $s_l^{\pi_l}$. Here s_l denotes the spin of the light degrees of freedom and π_l the parity. The D, D^* mesons are $L = 0$ negative parity mesons. The D_0^*, D_1^* and D_1, D_2^* are excited mesons with $L = 1$ and positive parity. \bar{m} refers to the average mass of the HQS doublet weighted by the number of helicity states [21].

We review some of the recent theoretical and experimental results for the above mentioned decays. Factorization theorems [9, 19] in SCET have been proven for $\bar{B} \rightarrow D^{(*)}M$ decays (including the often less understood color suppressed modes) to first non-vanishing order in Λ_{QCD}/Q . Here Q is a hard scale on the order of the bottom and charmed quark masses $m_{b,c}$ or the light meson energy E_M . It was shown that the C and E topologies are suppressed by Λ_{QCD}/Q relative to T which explains the observed [22] suppression of the $\bar{B}^0 \rightarrow D^{(*)0}M^0$ color suppressed modes. Using heavy quark symmetry in conjunction with factorization, quantitative model independent phenomenological results relating the D and D^* amplitudes were obtained

$$\frac{Br(\bar{B} \rightarrow D^*M)}{Br(\bar{B} \rightarrow DM)} = 1. \quad (1)$$

These results are to leading order in $\alpha_s(Q)$ and Λ_{QCD}/Q and hold true in the color allowed channels for all the above mentioned light mesons M [6]. For the color suppressed modes the predictions hold for $M = \pi, \rho, K, K_\parallel^*$ [19]. For the kaons in the color suppressed channels, there are additional non-perturbative functions from long distance operators which require the K^* 's to be longitudinally polarized for the prediction to hold. Predictions of the type in Eq. (1) have also been made for the case of the baryon decays [24] $\Lambda_b \rightarrow \Xi_c^{(*)}M$ and $\Lambda_b \rightarrow \Sigma_c^{(*)}M$ where heavy quark symmetry relates Ξ_c to Ξ_c^* and Σ_c to Σ_c^* . In this case the ratio of branching fractions was found to be 2.

The relation between the D and D^* amplitudes in Eq. (1) can be understood in terms of soft-collinear factorization and Heavy Quark Symmetry(HQS) [25, 26]. In the heavy quark limit $m_c \rightarrow \infty$ and in the absence of hard gluons, the D and D^* charmed mesons sit in a HQS doublet (D, D^*) . Members within a HQS doublet are distinguished by the coupling of the spin of the charmed quark with the spin of the light degrees of freedom (s_l) [27]. Their total spin is given by $J_\pm = s_l \pm \frac{1}{2}$. Since spin dependent chromomagnetic interactions are Λ_{QCD}/m_c suppressed, the D and D^* states are degenerate at leading order. However, the presence of collinear gluons in the energetic light meson can spoil HQS since chromomagnetic corrections of order E_M/m_c from such gluons are not suppressed. Factorization of these collinear modes from the soft degrees of freedom becomes crucial in restoring this symmetry. SCET provides us with such a factorization theorem where the amplitude factors into soft $\langle D^{(*)}| \dots |B \rangle$ and collinear $\langle M| \dots |0 \rangle$ matrix elements at leading order. One is now free to apply HQS in the soft sector and the result of Eq. (1) is a statement of this symmetry.

There exists a tower of HQS doublets for the charmed mesons where (D, D^*) sits at the base. The first three HQS doublets are listed in Table I. In this paper we extend the analysis

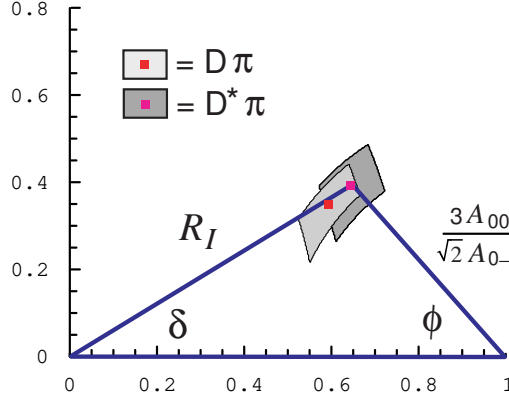


FIG. 2: The ratio of isospin amplitudes $R_I = A_{1/2}/(\sqrt{2}A_{3/2})$ and strong phases δ and ϕ in $\bar{B} \rightarrow D\pi$ and $\bar{B} \rightarrow D^*\pi$ taken from Ref. [28]. The central values following from the D and D^* data in Table I are denoted by squares, and the shaded regions are the 1σ ranges computed from the branching ratios. The overlap of the D and D^* regions shows that the prediction in Eq. (1) works well.

to the case where the final state charmed mesons are D_1 or D_2^* which sit in the third HQS doublet. A similar analysis can be done for the (D_0^*, D_1^*) doublet but these are difficult to observe due to their relatively broad width [27]. For this reason, we restrict our analysis to the (D_1, D_2^*) doublet.

For $M = \pi, \rho$ the final state can be decomposed into an isospin $I = 1/2, 3/2$ basis allowing us to parametrize the physical amplitudes in terms of the isospin amplitudes $A_{1/2}$ and $A_{3/2}$

$$\begin{aligned}
 A_{+-} &= A(\bar{B}^0 \rightarrow D^+ \pi^-) = \frac{1}{\sqrt{3}}A_{3/2} + \sqrt{\frac{2}{3}}A_{1/2} = T + E, \\
 A_{0-} &= A(B^- \rightarrow D^0 \pi^-) = \sqrt{3}A_{3/2} = T + C, \\
 A_{00} &= A(\bar{B}^0 \rightarrow D^0 \pi^0) = \sqrt{\frac{2}{3}}A_{3/2} - \frac{1}{\sqrt{3}}A_{1/2} = \frac{1}{\sqrt{2}}(C - E).
 \end{aligned} \tag{2}$$

These relations also hold true for D^{**} mesons in the final state. The relative phase between the isospin amplitudes is defined as $\delta = \arg(A_{1/2}A_{3/2}^*)$. The above equations can be brought into the form:

$$R_I + \frac{3A_{00}}{\sqrt{2}A_{0-}} = 1, \tag{3}$$

where $R_I = A_{1/2}/(2A_{3/2})$. This relation can be expressed as a triangle in the complex plane as shown in Fig. 2 for the $\bar{B} \rightarrow D^{(*)}\pi$ channels. The overall phase was chosen so that the A_{0-} amplitude is real. The angle ϕ is the non-perturbative strong phase of the color suppressed amplitude A_{00} . A novel mechanism for the generation of this phase was discussed in [19]. The prediction of Eq. (1) manifests itself as the identical overlap of the $D\pi$ and $D^*\pi$ isospin triangles i.e. $\delta = \delta^*$ and $\phi = \phi^*$. Fig. 2 shows the remarkable agreement of this prediction with data. For the $\bar{B} \rightarrow D^{**}M$ modes not enough data exists to construct analogous isospin triangles. However, the experimental scene is quite active with most recent measurements

in the color allowed sector giving the ratio

$$\frac{Br(B^- \rightarrow D_2^{*0}\pi^-)}{Br(B^- \rightarrow D_1^0\pi^-)} = 0.79 \pm 0.11, \quad (4)$$

obtained after averaging the Belle [29] and Babar [30] data. In this paper, we shed light on this ratio and also make predictions in the color suppressed sector.

In extending the analysis to include excited charmed mesons, the constraint of HQS introduces possible complications in the power counting scheme. HQS requires the matrix elements of the weak current between B and (D_1, D_2^*) to vanish at zero recoil [31]. This requires that they be proportional to some positive power of $(\omega - 1)$ at leading order in Λ_{QCD}/Q . Here $\omega = v \cdot v'$ where v and v' are the velocities of the bottom and charm quarks respectively and $v^2 = v'^2 = 1$. For semileptonic decays this means that HQS breaking Λ_{QCD}/Q corrections can compete with the leading order prediction [21, 24]. For example, if the amplitude were to have the generic form

$$A(\omega) \sim (\omega - 1)[1 + \Lambda_{QCD}/Q + \dots] + [0 + \Lambda_{QCD}/Q + \dots], \quad (5)$$

and $(\omega - 1) \sim \Lambda_{QCD}/Q$, then the subleading Λ_{QCD}/Q terms in the second square bracket are of the same order as the leading order terms in the first square bracket. The effect of the subleading corrections is especially important near zero recoil where $\omega \rightarrow 1$. The two body decays $\bar{B} \rightarrow (D_1, D_2^*)M$ occur at maximum recoil where $(\omega_0 - 1) \sim 0.3$ which is numerically of the same order as Λ_{QCD}/Q . One is thus forced to consider the role of subleading corrections and how they compare with the leading order predictions. However, we will see that maximum recoil is a special kinematic point at which the constraint of HQS enters in a very specific manner so as to preserve the Λ_{QCD}/Q power counting scheme. The main results of this paper are

- At leading order, the ideas of factorization, generation of non-perturbative strong phases, and the relative Λ_{QCD}/Q suppression of the color suppressed modes are the same for B -decays to excited charmed mesons $\bar{B} \rightarrow D^{**}M$ and to ground state charmed mesons $\bar{B} \rightarrow D^{(*)}M$.
- The constraint of HQS takes on a different character at maximum recoil compared to expectations from the analysis of semileptonic decays near zero recoil. In particular, at maximum recoil there is no suppression of the leading order contribution due to HQS. Thus, the SCET/HQET power counting scheme remains intact and allows us to rely on leading order predictions up to corrections suppressed by at least Λ_{QCD}/Q . We verify this explicitly for subleading corrections to the semileptonic form factors at maximum recoil.
- At leading order, factorization combined with HQS predicts the equality of the $\bar{B} \rightarrow D_1 M$ and $\bar{B} \rightarrow D_2^* M$ branching fractions and their strong phases. In the color suppressed sector, this prediction is quite non-trivial from the point of naive factorization since the tensor meson D_2^* cannot be created via a V-A current.
- Recent data [29, 30] reports a 20% deviation of the ratio of branching fractions from unity in the color allowed sector. The subleading corrections of order Λ_{QCD}/Q are expected to be of this same size and could explain this deviation from unity.

In section II we review the analysis of SCET for $\bar{B} \rightarrow D^{(*)}M$. At leading order, most of the results can be identically carried over to the analysis for the excited HQS doublet (D_1, D_2^*). In section III we consider the effect of subleading corrections and phenomenological results are given in section IV.

II. SOFT COLLINEAR EFFECTIVE THEORY FOR $\bar{B} \rightarrow D^{(*)}M$

Observing the decay in the rest frame of the B meson, one can identify two types of degrees of freedom with offshellness $p^2 \sim \Lambda_{QCD}^2$ that are responsible for binding the hadrons. These are the collinear $(p^+, p^-, p_\perp) \sim Q(\eta^2, 1, \eta)$ and soft $(p^+, p^-, p_\perp) \sim Q(\eta, \eta, \eta)$ degrees of freedom where $\eta \sim \Lambda_{QCD}/Q$. The formalism of SCET allows us to construct an effective theory of this process directly in terms of these relevant soft and collinear modes with all other offshell modes integrated out. This effective theory at the hadronic scale is given the name SCET_{II}¹.

The $\bar{B} \rightarrow D^{(*)}M$ processes receive contributions from various effects occurring at different distance scales. A complete description of these decays requires us to flow between effective theories from the electroweak scale down to the hadronic scale. Each effective theory along the way contributes the necessary mechanism for the decay to proceed. These mechanisms are encoded as effective operators with appropriate Wilson coefficients in the next effective theory on our way down to SCET_{II} at the hadronic scale.

The $b \rightarrow c$ quark flavor changing process occurs at the electroweak scale ($p^2 \sim m_W^2$) through a W -exchange process. The W boson is then integrated out to give the effective Hamiltonian

$$\mathcal{H}_W = \frac{G_F}{\sqrt{2}} V_{cb} V_{ud}^* [C_1(\mu)(\bar{c}b)_{V-A}(\bar{d}u)_{V-A} + C_2(\mu)(\bar{c}_i b_j)_{V-A}(\bar{d}_j u_i)_{V-A}], \quad (6)$$

where i, j are color indices, and for $\mu_b = 5$ GeV, $C_1(\mu_b) = 1.072$ and $C_2(\mu_b) = -0.169$ at NLL order in the NDR scheme [35]. This Hamiltonian gives rise to the three distinct topologies through which the decay can proceed as shown in Fig. 1.

Next we would like to match H_W onto operators in SCET_{II} with soft and collinear degrees of freedom. However, the soft-collinear interactions produce offshell modes $p^2 \sim Q\Lambda_{QCD}$ that are not present in SCET_{II}. These modes have momentum scalings $(p^+, p^-, p_\perp) \sim Q(\eta, 1, \eta)$ and have to be integrated out [18]. Instead, it becomes more convenient to go through an intermediate effective theory SCET_I [36] at the scale $Q\Lambda_{QCD}$ and do the matching in two steps. SCET_I is a theory of ultrasoft $(p^+, p^-, p_\perp) \sim Q(\lambda^2, \lambda^2, \lambda^2)$ and hard-collinear $(p^+, p^-, p_\perp) \sim Q(\lambda^2, 1, \lambda)$ modes where $\lambda = \sqrt{\eta} = \sqrt{\frac{\Lambda_{QCD}}{Q}}$. The ultrasoft modes are identical to the soft modes and the hard-collinear modes play the role of the offshell modes produced by the soft-collinear interactions in SCET_{II}. The hard-collinear modes are eventually matched onto the collinear modes of SCET_{II}. This two step matching procedure allows us to avoid dealing directly with non-local interactions, although it is also possible to construct SCET_{II} directly from QCD [38]. In summary, one arrives at the effective theory

¹ The soft-collinear messenger modes of Ref. [32] could play a role in subleading corrections which we will not consider. The nature of these messenger modes is still unclear due to their dependence on the choice of infrared regulator [33, 34].

Theory	Scale	Wilson Coefficients	Physics Effect
SM	$\mu^2 \sim m_W^2$	-	$b \rightarrow c$ quark flavor transition
H_W	$\mu^2 \sim Q^2$	C_1, C_2	W boson integrated out
SCET _I	$\mu^2 \sim Q\Lambda_{QCD}$	C_L, C_R	soft-collinear transitions
SCET _{II}	$\mu^2 \sim \Lambda_{QCD}^2$	J	binding of hadrons

TABLE II: The effective theories at different distance scales and the effects they provide for the $B \rightarrow DM$ process to occur. The Wilson coefficients that show up in each theory are also given.

SCET_{II} at the hadronic scale through a series of matching and running procedures starting with the Standard Model(SM)

$$SM \rightarrow H_W \rightarrow SCET_I \rightarrow SCET_{II}.$$

In the above chain of effective theories, each matching calculation introduces Wilson coefficients which encode the physics of harder scales. These ideas are summarized in Table II and are illustrated in Fig. 3. We now briefly review the details of the procedure just discussed.

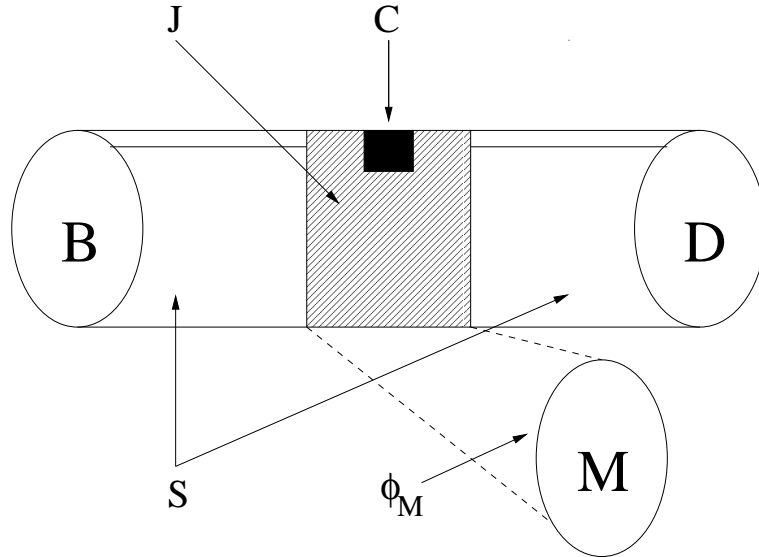


FIG. 3: A schematic representation of the $B \rightarrow DM$ process and the contributions it receives from effects at different distance scales. The shaded black box is the weak vertex where the $b \rightarrow c$ transition takes place, the shaded grey region is where soft spectator quarks are converted to collinear quarks that end up in the light meson, and the unshaded regions are where non-perturbative processes responsible for binding of hadrons take place. These regions correspond to the functions C , J , S , and ϕ_M as labeled in the figure. For the color allowed modes, where the light meson is produced directly at the weak vertex and no soft-collinear transitions involving the spectator quarks are required, the jet function J is trivially just one.

1. Color Allowed Modes

The leading order contribution to color allowed modes comes via the T topology (see Fig. 1) where the final state light meson is emitted directly at the weak vertex. After the W boson is integrated out we arrive at the effective Hamiltonian H_W in Eq. (6). Next, we match H_W onto SCET_I :

$$\sum_{1,2} C_i O_i \rightarrow 4 \sum_{j=L,R} \int d\tau_1 d\tau_2 [C_j^{(0)}(\tau_1, \tau_2) \mathcal{Q}_j^{(0)}(\tau_1, \tau_2) + C_j^{(8)}(\tau_1, \tau_2) \mathcal{Q}_j^{(8)}(\tau_1, \tau_2)], \quad (7)$$

where the O_i refer to the four quark operators in Eq. (6) and the prefactor $\frac{G_F}{\sqrt{2}} V_{cb} V_{ud}^*$ has been dropped from both sides of the equation. At leading order in SCET_I there are four operators [$j = L, R$]

$$\begin{aligned} \mathcal{Q}_j^{(0)}(\tau_1, \tau_2) &= [\bar{h}_{v'}^{(c)} \Gamma_j^h h_v^{(b)}] [(\bar{\xi}_n^{(d)} W)_{\tau_1} \Gamma_n (W^\dagger \xi_n^{(u)})_{\tau_2}], \\ \mathcal{Q}_j^{(8)}(\tau_1, \tau_2) &= [\bar{h}_{v'}^{(c)} Y \Gamma_j^h T^a Y^\dagger h_v^{(b)}] [(\bar{\xi}_n^{(d)} W)_{\tau_1} \Gamma_n T^a (W^\dagger \xi_n^{(u)})_{\tau_2}]. \end{aligned} \quad (8)$$

The superscript $(0, 8)$ denotes the $1 \otimes 1$ and $T^a \otimes T^a$ color structures. The Dirac structures on the heavy side are $\Gamma_{L,R}^h = \not{p} P_{L,R}$ with $P_{R,L} = \frac{1}{2}(1 \pm \gamma_5)$, while on the hard-collinear side we have $\Gamma_n = \not{p} P_L/2$. The momenta labels are defined by $(W^\dagger \xi_n)_{\omega_2} = [\delta(\omega_2 - \bar{P}) W^\dagger \xi_n]$. The tree level matching conditions are:

$$C_L^{(0)}(\tau_i) = C_1 + \frac{C_2}{N_c}, \quad C_L^{(8)}(\tau_i) = 2C_2, \quad C_R^{(0,8)}(\tau_i) = 0. \quad (9)$$

Matching corrections of order $\mathcal{O}(\alpha_s)$ can be found in Ref. [7].

The operators in Eq. (8) are written in terms of hard-collinear fields which do not couple to usoft particles at leading order. This was achieved by a decoupling field redefinition [18] on the hard-collinear fields $\xi_n \rightarrow Y \xi_n$ etc. The operators in Eq. (8) are then matched onto SCET_{II} to give $[\omega_i = \tau_i]$

$$\begin{aligned} \mathcal{Q}_j^{(0)}(\omega_1, \omega_2) &= [\bar{h}_{v'}^{(c)} \Gamma_j^h h_v^{(b)}] [(\bar{\xi}_n^{(d)} W)_{\omega_1} \Gamma_n (W^\dagger \xi_n^{(u)})_{\omega_2}], \\ \mathcal{Q}_j^{(8)}(\omega_1, \omega_2) &= [\bar{h}_{v'}^{(c)} S \Gamma_j^h T^a S^\dagger h_v^{(b)}] [(\bar{\xi}_n^{(d)} W)_{\omega_1} \Gamma_n T^a (W^\dagger \xi_n^{(u)})_{\omega_2}], \end{aligned} \quad (10)$$

where W and S are the hard-collinear and soft Wilson lines respectively. As mentioned earlier, the hard-collinear fields of SCET_I in Eq. (8) match onto the collinear fields of SCET_{II} in Eq. (10). The ultrasoft modes of SCET_I match onto the soft modes of SCET_{II} since these are identical. Note that since the collinear quarks in the pion are produced directly at the weak vertex, the jet functions $J^{(0,8)}$ which are the Wilson coefficients that arise in matching SCET_I onto SCET_{II} are just one.

At leading order in Λ_{QCD}/Q only the operators $\mathcal{Q}_{L,R}^{(0)}$ and the leading order collinear and soft Lagrangians ($\mathcal{L}_c^{(0)}$, $\mathcal{L}_s^{(0)}$), contribute to the $B^- \rightarrow D^{(*)0} \pi^-$ and $\bar{B}^0 \rightarrow D^{(*)+} \pi^-$ matrix elements. The matrix elements of $\mathcal{Q}_{L,R}^{(8)}$ vanish because they factorize into a product of bilinear matrix elements and the octet currents give vanishing contribution between color singlet states [9]. Since the soft and collinear modes are decoupled at leading order, the matrix elements of $\mathcal{Q}_{L,R}^{(0)}$ factorize into a soft $B \rightarrow D$ matrix element and a light cone pion wave function. By employing the trace formalism of HQET on the soft sector, the factorized

amplitude for the color allowed modes to all orders in $\alpha_s(Q)$ and to leading order in Λ_{QCD}/Q can now be written as:

$$A(B \rightarrow D^{(*)}\pi) = N^{(*)} \xi(w_0, \mu) \int_0^1 dx T^{(*)}(x, m_c/m_b, \mu) \phi_\pi(x, \mu), \quad (11)$$

where normalization factor is given by

$$N^{(*)} = \frac{G_F V_{cb} V_{ud}^*}{\sqrt{2}} E_\pi f_\pi \sqrt{m_{D^{(*)}} m_B} \left(1 + \frac{m_B}{m_{D^{(*)}}}\right). \quad (12)$$

$\phi_\pi(x, \mu)$ is the non-perturbative pion light cone wave function, and $\xi(w_0, \mu)$ is the Isgur-Wise function evaluated at maximum recoil. The hard coefficient $T^{(*)}(x, \mu) = C_{L\pm R}^{(0)}((4x-2)E_\pi, \mu, m_b)$, where the \pm correspond to the D and D^* respectively, and $C_{L\pm R}^{(0)} = C_L^{(0)} \pm C_R^{(0)}$. With $C_R^{(0)} = 0$ at leading order in $\alpha_s(Q)$ we have $T(x, \mu) = T^*(x, \mu)$. In addition, in the heavy quark limit $N = N^*$ and one is led to the result in Eq. (1) for the color allowed modes.

2. Color Suppressed Modes

For the color suppressed modes the T topology does not contribute since the W boson cannot produce the appropriate quark flavors needed to produce a neutral light meson at the weak vertex. These modes receive contributions only from the C and E topologies where spectator quarks from the bottom or charmed mesons end up in the pion. As in the case of the color allowed modes, after the W boson is integrated out, the weak vertex Hamiltonian H_W is matched onto the SCET_I operators $\mathcal{Q}_j^{(0,8)}(\tau_1, \tau_2)$. However, in this case to produce a neutral collinear light meson and a charmed meson with soft degrees of freedom, SCET_I requires a T-ordered product that involves two soft-hard-collinear transitions. SCET_I provides such a T-ordered product that involves two insertions of the subleading ultrasoft-hard-collinear Lagrangian $\mathcal{L}_{\xi q}^{(1)}$:

$$T_j^{(0,8)} = \frac{1}{2} \int d^4x d^4y T\{\mathcal{Q}_j^{(0,8)}(0), i\mathcal{L}_{\xi q}^{(1)}(x), i\mathcal{L}_{\xi q}^{(1)}(y)\}. \quad (13)$$

Here the subleading Lagrangian is [36, 37]

$$\mathcal{L}_{\xi q}^{(1)} = (\bar{\xi}_n W) \left(\frac{1}{\mathcal{P}} W^\dagger i g \not{B}_\perp W \right) q_{us} - \bar{q}_{us} \left(W^\dagger i g \not{B}_\perp W \frac{1}{\mathcal{P}^\dagger} \right) (W^\dagger \xi_n), \quad (14)$$

where $i g \not{B}_\perp = [i \bar{n} \cdot D^c, i \not{D}_\perp^c]$. The two factors of $i\mathcal{L}_{\xi q}^{(1)}$ in Eq. (13) are necessary to swap one u quark and one d quark from ultrasoft to intermediate collinear as shown in Fig. 4(a, b). In contrast to the T topology, for this case both the $\mathcal{Q}_j^{(0)}$ and $\mathcal{Q}_j^{(8)}$ color structures can contribute. By power counting, the $T_j^{(0,8)}$'s are suppressed by $\lambda^2 = \Lambda/Q$ relative to the leading operators for the T topology.

The SCET_I diagrams are now matched onto operators in SCET_{II}. These are shown in Fig. 4(b, c, d). In Figs. 4a,b the gluon always has offshellness $p^2 \sim E_M \Lambda$ due to momentum conservation, and is shrunk to a point in SCET_{II}. However, the collinear quark propagator in (a,b) can either have $p^2 \sim E_M \Lambda$ giving rise to the short distance SCET_{II} contribution

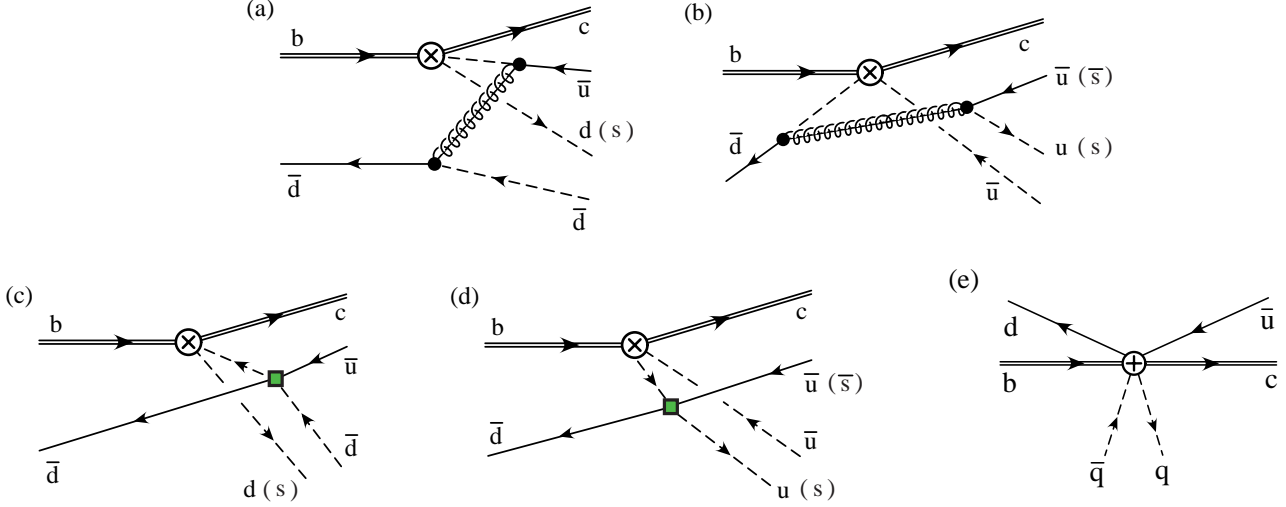


FIG. 4: Graphs for the tree level matching calculation from SCET_I (a,b) onto SCET_{II} (c,d,e) taken from Ref. [19]. The dashed lines are collinear quark propagators and the spring with a line is a collinear gluon. Solid lines in (a,b) are ultrasoft and those in (c,d,e) are soft. The \otimes denotes an insertion of the weak operator, given in Eq. (8) for (a,b) and in Eq. (10) in (c,d). The \oplus in (e) is a 6-quark operator from Eq. (15). The two solid dots in (a,b) denote insertions of the mixed usoft-collinear quark action $\mathcal{L}_{\xi q}^{(1)}$. The boxes denote the SCET_{II} operator $\mathcal{L}_{\xi \xi q q}^{(1)}$ [19].

in Fig. 4e, or it can have $p^2 \sim \Lambda^2$ which gives the long distance SCET_{II} contribution in Figs. 4c,d. It was shown [19] to leading order in $\alpha_s(Q)$ that the long distance contributions vanish for $M = \pi, \rho$. For the kaons, these long distance contributions are non-vanishing but were shown to be equal for $\bar{B} \rightarrow D\bar{K}$ and $\bar{B} \rightarrow D^*\bar{K}$ and for $\bar{B} \rightarrow D\bar{K}_\parallel^*$ and $\bar{B} \rightarrow D^*\bar{K}_\parallel^*$. In this section, we only review the analysis for $M = \pi, \rho$ and refer the reader to Ref. [19] for the kaon analysis. Expressions for the long distance contributions are given in Ref. [19]. To all orders in perturbation theory the Wilson coefficients $J^{(0,8)}$ from the matching of SCET_I \rightarrow SCET_{II} generate only one spin structure and two color structures for the SCET_{II} short distance six quark operator:

$$\begin{aligned} O_j^{(0)}(k_i^+, \omega_k) &= \left[\bar{h}_{v'}^{(c)} \Gamma_j^h h_v^{(b)} (\bar{d} S)_{k_1^+} \not{p} P_L (S^\dagger u)_{k_2^+} \right] \left[(\bar{\xi}_n W)_{\omega_1} \Gamma_c (W^\dagger \xi_n)_{\omega_2} \right], \\ O_j^{(8)}(k_i^+, \omega_k) &= \left[(\bar{h}_{v'}^{(c)} S) \Gamma_j^h T^a (S^\dagger h_v^{(b)}) (\bar{d} S)_{k_1^+} \not{p} P_L T^a (S^\dagger u)_{k_2^+} \right] \left[(\bar{\xi}_n W)_{\omega_1} \Gamma_c (W^\dagger \xi_n)_{\omega_2} \right], \end{aligned} \quad (15)$$

where the $d, u, h_{v'}^{(c)}$, and $h_v^{(b)}$ fields are soft, and the ξ_n fields are collinear isospin doublets, $(\xi_n^{(u)}, \xi_n^{(d)})$. In Eq. (15) $\Gamma_{L,R}^h = \not{p} P_{L,R}$ as in Eq. (8), while for the collinear isospin triplet $\Gamma_c = \tau^3 \not{p} P_L/2$. We do not list operators with a T^a next to Γ_c since they will give vanishing contribution in the collinear matrix element. The matrix elements of these operators gives the final result for the color suppressed amplitude:

$$\begin{aligned} A_{00}^{D(*)} &= N_0^M \int_0^1 dx dz \int dk_1^+ dk_2^+ \left[C_L^{(i)}(z) J^{(i)}(z, x, k_1^+, k_2^+) S_L^{(i)}(k_1^+, k_2^+) \phi_M(x) \right] \\ &\quad \pm C_R^{(i)}(z) J^{(i)}(z, x, k_1^+, k_2^+) S_R^{(i)}(k_1^+, k_2^+) \phi_M(x) \right], \end{aligned} \quad (16)$$

where we sum over the color structures $i = 0, 8$ and \pm refers to D and D^* respectively. The coefficients $C_{L,R}^{(0,8)}$ and $J^{(0,8)}$ are Wilson coefficients that arise in matching calculations from $H_W \rightarrow \text{SCET}_I$ and $\text{SCET}_I \rightarrow \text{SCET}_{II}$ respectively. Tree level expressions for $J^{(0,8)}$ are given in Eq.(42) of Ref. [19]. The non-perturbative functions $S_{L,R}$ are given by

$$\begin{aligned} \frac{\langle D^0(v') | (\bar{h}_{v'}^{(c)} S) \not{p} P_{L,R}(S^\dagger h_v^{(b)}) (\bar{d} S)_{k_1^+} \not{p} P_L(S^\dagger u)_{k_2^+} | \bar{B}^0(v) \rangle}{\sqrt{m_B m_D}} &= S_{L,R}^{(0)}(k_j^+), \\ \frac{\langle D^{*0}(v', \varepsilon) | (\bar{h}_{v'}^{(c)} S) \not{p} P_{L,R}(S^\dagger h_v^{(b)}) (\bar{d} S)_{k_1^+} \not{p} P_L(S^\dagger u)_{k_2^+} | \bar{B}^0(v) \rangle}{\sqrt{m_B m_{D^*}}} &= \pm \frac{n \cdot \varepsilon^*}{n \cdot v'} S_{L,R}^{(0)}(k_j^+). \end{aligned} \quad (17)$$

Finally, the light cone wave functions are given by [we suppress pre-factors of $\int_0^1 dx \delta(\omega_1 - x \bar{n} \cdot p_M) \delta(\omega_2 + (1-x) \bar{n} \cdot p_M)$ on the RHS]²

$$\begin{aligned} \langle \pi_n^0 | (\bar{\xi}_n W)_{\omega_1} \not{p} \gamma_5 \tau_3 (W^\dagger \xi_n)_{\omega_2} | 0 \rangle &= -i \sqrt{2} f_\pi \bar{n} \cdot p_\pi \phi_\pi(\mu, x), \\ \langle \rho_n^0(\varepsilon) | (\bar{\xi}_n W)_{\omega_1} \not{p} \tau_3 (W^\dagger \xi_n)_{\omega_2} | 0 \rangle &= i \sqrt{2} f_\rho \bar{n} \cdot p_\rho \phi_\rho(\mu, x). \end{aligned} \quad (18)$$

With $C_R = 0$ at leading order in $\alpha_s(Q)$ in Eq. (16) we arrive at the result in Eq. (1) for the color suppressed modes.

III. EXCITED CHARMED MESONS

Eqs. (11) and (16) are the main results of the analysis for the $B \rightarrow D^{(*)} M$ decays. The analysis for decays with excited charmed mesons $B \rightarrow D^{**} M$ will proceed in exactly the same manner. Any difference in results will show up only at the non-perturbative scale i.e. in SCET_{II} . In other words, the doublets (D, D^*) and (D_1, D_2^*) have the same quark content and any difference between them arises only from non-perturbative effects responsible for their binding. The physics at the scales $\mu^2 \sim m_W^2$, Q^2 , and $Q \Lambda_{QCD}$ or in the theories SM , H_W , and SCET_I is the same leaving the perturbative functions $C_{1,2}$, $C_{L,R}^{(0,8)}$, and $J^{(0,8)}$ unchanged (see Fig. 3). The light cone wave function ϕ_M will also remain unchanged since the same final state light meson appears. At leading order, the only change will be in the soft functions $S_{L,R}^{(i)}$ and ξ since the matrix elements will now involve different non-perturbative final states namely (D_1, D_2^*) . We will denote the modified functions as $Q_{L,R}^{(i)}$ and τ corresponding to $S_{L,R}^{(i)}$ and ξ respectively.

A. Leading Order Predictions

We now begin our analysis for the excited charmed states. We start by obtaining the modified soft functions τ and $Q_{L,R}^{(i)}$ and then carry over results for the perturbative functions and the non-perturbative collinear sector from the previous section to obtain the analog of Eqs. (11) and (16).

² Our vector meson states are defined with an extra minus sign relative to the standard convention.

1. Color Allowed Modes

We first analyze the soft functions for the color allowed modes $\bar{B}^0 \rightarrow (D_1^+, D_2^{*+})M^-$ and $B^- \rightarrow (D_1^0, D_2^{*0})M^-$. As before, the leading contribution to these modes comes from the T topology which is given by the matrix elements of the effective SCET_{II} operators $\mathcal{Q}_{L,R}^{(0,8)}$ of Eq. (10). These matrix elements factorize into soft and collinear sectors. Using the formalism of HQET, the soft part of the matrix element can be expressed in general form as a trace

$$\frac{\langle D_2^*, D_1(v') | \bar{h}_{v'}^{(c)} \Gamma_{L,R}^h h_v^{(b)} | \bar{B}^0(v) \rangle}{\sqrt{m_B m_D}} = \tau(\omega) \text{Tr} [v_\sigma \bar{F}_{v'}^{(c)\sigma} \Gamma H_v^{(b)}], \quad (19)$$

where $\tau(\omega)$ is a new Isgur-Wise function analogous to $\xi(\omega)$. As in the case of ground state charmed mesons, the operators $\mathcal{Q}_{L,R}^{(8)}$ give vanishing contribution. $H_v^{(b)}$ and $F_{v'}^{(c)\sigma}$ in Eq. (19) are the superfields for the heavy meson doublets (\bar{B}, \bar{B}^*) and (D_1, D_2^*) respectively [39]

$$\begin{aligned} H_v &= \frac{1 + \not{v}}{2} (P_v^{*\mu} \gamma_\mu + P_v \gamma_5) \\ F_v^\sigma &= \frac{1 + \not{v}}{2} (D_2^{*\sigma\nu} \gamma_\nu - \sqrt{\frac{3}{2}} D_1^\nu \gamma_5 [g_\nu^\sigma - \frac{1}{3} \gamma_\nu (\gamma^\sigma - v^\sigma)]). \end{aligned} \quad (20)$$

As mentioned in the introduction, the matrix element in Eq. (19) which also appears in the case of semileptonic decays must vanish in the limit of zero recoil. This condition is manifest in the right hand side of Eq. (19) through the property $v'_\sigma \bar{F}_{v'}^{(c)\sigma} = 0$. Thus, we expect the leading order amplitude to be proportional to some positive power of $(\omega - 1)$. At maximum recoil $(\omega_0 - 1) \sim 0.3 \sim \Lambda_{QCD}/Q$ putting $(\omega_0 - 1)$ and Λ_{QCD}/Q on the same footing in the power counting scheme. In addition, maximum recoil is a special kinematic point where the heavy meson masses are related to ω_0 through $(\omega_0 - 1) = \frac{(m_B - m_D)^2}{2m_B m_D}$. We must keep this relation in mind to make the power counting manifest and so it becomes convenient to express $(m_B - m_D)$ in terms of $(\omega_0 - 1)$.

Computing the trace in Eq. (19) we arrive at the result

$$\begin{aligned} \frac{\langle D_1(v') | \bar{h}_{v'}^{(c)} \Gamma_{L,R}^h h_v^{(b)} | \bar{B}^0(v) \rangle}{\sqrt{m_B m_D}} &= \tau(\omega) \sqrt{\frac{m_B(\omega + 1)}{3m_D}} \epsilon^* \cdot v \\ \frac{\langle D_2^*(v') | \bar{h}_{v'}^{(c)} \Gamma_{L,R}^h h_v^{(b)} | \bar{B}^0(v) \rangle}{\sqrt{m_B m_D}} &= \pm \tau(\omega) \sqrt{\frac{m_B}{2m_D(\omega - 1)}} \epsilon^{*\sigma\nu} v_\sigma v_\nu, \end{aligned} \quad (21)$$

where the \pm for the D_2^* refer to the choice of Γ_L^h and Γ_R^h Dirac structures respectively. ϵ^μ and $\epsilon^{\mu\nu}$ are the polarizations for D_1 and D_2^* respectively. Combining this result for the soft

sector with the hard and collinear parts from the previous section we obtain the final result

$$\begin{aligned}
A(B \rightarrow D_1 M) &= N^{D1} E_M \sqrt{\frac{m_B(\omega_0 + 1)}{3m_D}} \epsilon^* \cdot v \tau(w_0, \mu) \\
&\quad \times \int_0^1 dx T^{D_1}(x, m_c/m_b, \mu) \phi_M(x, \mu) \\
A(B \rightarrow D_2^* M) &= N^{D2*} E_M \sqrt{\frac{m_B}{2m_D(\omega_0 - 1)}} \epsilon^{*\sigma\nu} v_\sigma v_\nu \tau(w_0, \mu) \\
&\quad \times \int_0^1 dx T^{D_2^*}(x, m_c/m_b, \mu) \phi_M(x, \mu),
\end{aligned} \tag{22}$$

where the normalizations are given by

$$N^{D1} = \frac{G_F V_{cb} V_{ud}^*}{\sqrt{2}} f_M \sqrt{m_B m_{D1}}, \quad N^{D2*} = \frac{G_F V_{cb} V_{ud}^*}{\sqrt{2}} f_M \sqrt{m_B m_{D2*}} \tag{23}$$

and the hard kernels $T^{(D_1, D_2^*)}(x, \mu)$ are the same as those appearing in Eq. (11) $T^{(D_1, D_2^*)}(x, \mu) = T^{(*)}(x, \mu)$. Using the properties of the polarization sums

$$\sum_{pol} |\epsilon^* \cdot v|^2 = (\omega + 1)(\omega - 1), \quad \sum_{pol} |\epsilon^{*\sigma\nu} v_\sigma v_\nu|^2 = \frac{2}{3}(\omega + 1)^2(\omega - 1)^2, \tag{24}$$

the unpolarized amplitude squared is given by

$$\begin{aligned}
\sum_{pol} |A(B \rightarrow (D_1, D_2^*) M)|^2 &= |N^{(D1, D2*)} \int_0^1 dx T^{(D1, D_2^*)}(x, m_c/m_b, \mu) \phi_M(x, \mu)|^2 \\
&\quad \times \frac{m_B \tau^2(\omega, \mu)}{3m_D} (\omega_0 + 1)^2 (\omega_0 - 1).
\end{aligned} \tag{25}$$

At leading order in $\Lambda_{QCD}/m_{b,c}$ the masses in the heavy quark doublet (D_1, D_2^*) are degenerate giving the relation $N^{(D1)} = N^{(D2*)}$. In addition at leading order in $\alpha_s(Q)$, $T^{(D1)} = T^{(D2*)}$ allowing us to make a prediction for the unpolarized color allowed branching ratios:

$$\frac{Br(\bar{B}^0 \rightarrow D_2^{*+} M^-)}{Br(\bar{B}^0 \rightarrow D_1^+ M^-)} = \frac{Br(B^- \rightarrow D_2^{*0} M^-)}{Br(B^- \rightarrow D_1^0 M^-)} = 1. \tag{26}$$

The same result was derived in ref. [21] at lowest order in $1/m_{b,c}$ by evaluating their results for semileptonic decays at the maximum recoil point and replacing the $e\bar{\nu}$ pair with a massless pion. Recently, a theoretical prediction of 0.91 for the above ratio was made in the covariant light front model [40].

2. Color Suppressed Modes

Now we look at the color suppressed modes $\bar{B}^0 \rightarrow (D_1^0, D_2^{*0}) M^0$. The leading contributions are from the C and E topologies which are given by matrix elements of the SCET_{II} operators $O_j^{(0,8)}(k_i^+, \omega_k)$ of Eq. (15). Once again, the result factorizes and using the formalism of HQET, the soft part of the matrix element can be expressed as a trace

$$\frac{\langle D_2^{(*)0}, D_1^0(v') | (\bar{h}_{v'}^{(c)} S) \Gamma_j^h (S^\dagger h_v^{(b)}) (\bar{d} S)_{k_1^+} \not{p} P_L (S^\dagger u)_{k_2^+} | \bar{B}^0(v) \rangle}{\sqrt{m_B m_D}} = \text{Tr} [\bar{F}_{v'}^{(c)\sigma} \Gamma_j^h H_v^{(b)} X_\sigma^{(0)}], \quad (27)$$

with similar expressions for the $O_j^{(8)}(k_i^+, \omega_k)$ operators. The Dirac structure $X_\sigma^{(0,8)}$ is of the most general form allowed by the symmetries of QCD and involves eight form factors

$$\begin{aligned} X_\sigma^{(0,8)} = & v_\sigma (a_1^{(0,8)} \not{p} P_L + a_2^{(0,8)} \not{p} P_R + a_3^{(0,8)} P_L + a_4^{(0,8)} P_R) \\ & + n_\sigma (a_5^{(0,8)} \not{p} P_L + a_6^{(0,8)} \not{p} P_R + a_7^{(0,8)} P_L + a_8^{(0,8)} P_R) \end{aligned} \quad (28)$$

Computing the trace in Eq. (27), the soft matrix elements are given by

$$\begin{aligned} \frac{\langle D_2^{*0}(v') | (\bar{h}_{v'}^{(c)} S) \Gamma_{L,R}^h (S^\dagger h_v^{(b)}) (\bar{d} S)_{k_1^+} \not{p} P_L (S^\dagger u)_{k_2^+} | \bar{B}^0(v) \rangle}{\sqrt{m_B m_D}} &= \frac{(\mp \epsilon^{*\sigma\nu} v_\sigma v_\nu) Q_{L,R}^{(0)}}{4(\omega+1)(\omega-1)} \\ \frac{\langle D_1^0(v') | (\bar{h}_{v'}^{(c)} S) \Gamma_{L,R}^h (S^\dagger h_v^{(b)}) (\bar{d} S)_{k_1^+} \not{p} P_L (S^\dagger u)_{k_2^+} | \bar{B}^0(v) \rangle}{\sqrt{m_B m_D}} &= \frac{(\epsilon^* \cdot v) Q_{L,R}^{(0)}}{\sqrt{24(\omega+1)(\omega-1)}} \end{aligned} \quad (29)$$

where,

$$\begin{aligned} Q_L^{(0)} &= \frac{-1}{m_B^2 m_D^2} [2m_B m_D (2a_1^{(0)} m_B^2 - a_3^{(0)} m_B^2 - a_4^{(0)} m_B m_D) \sqrt{(\omega+1)(\omega-1)} \\ &\quad + 4a_5^{(0)} m_B^4 - 2a_7^{(0)} m_B^4 - 2a_8^{(0)} m_D m_B^3] \\ Q_R^{(0)} &= \frac{-1}{m_B^2 m_D^2} [2m_B m_D (2a_2^{(0)} m_B^2 - a_3^{(0)} m_B m_D - a_4^{(0)} m_B^2) \sqrt{(\omega+1)(\omega-1)} \\ &\quad + 4a_6^{(0)} m_B^4 - 2a_7^{(0)} m_D m_B^3 - 2a_8^{(0)} m_B^4], \end{aligned} \quad (30)$$

with similar expressions for $Q_{L,R}^{(8)}$. Here the soft functions $Q_{L,R}^{(0,8)}$ are the analog of $S_{L,R}^{(0,8)}$ in Eq. (16). It was shown [19] that these soft functions generate a non-perturbative strong phase. We note that in both the D_1 and D_2^* decay channels, since the same moments of the non-perturbative functions $Q_{L,R}^{(0,8)}$ appear, their strong phases are predicted to be equal

$$\phi_{D_1 M} = \phi_{D_2^* M}. \quad (31)$$

The analogous strong phase ϕ for $\bar{B}^0 \rightarrow D^{(*)0} \pi^0$ is shown in Fig. 2. Since the strong phases ϕ and $\phi_{D_1 \pi, D_2^* \pi}$ are determined by different non-perturbative functions $S_{L,R}^{(0,8)}$ and $Q_{L,R}^{(0,8)}$ respectively, we do not expect them to be related.

Keeping in mind that the perturbative functions $C_{L,R}^{(i)}$ and $J^{(i)}$ remain unchanged, we can combine the result in Eq. (29) for soft sector with the collinear and hard parts of the amplitude to arrive at the result

$$\begin{aligned} A_{00}^{(D1)} &= \frac{-N^{D_1} \epsilon^* \cdot v}{\sqrt{24(\omega_0+1)(\omega_0-1)}} \int_0^1 dx dz \int dk_1^+ dk_2^+ \left[C_L^{(i)}(z) J^{(i)}(z, x, k_1^+, k_2^+) Q_L^{(i)}(k_1^+, k_2^+) \phi_M(x) \right. \\ &\quad \left. - C_R^{(i)}(z) J^{(i)}(z, x, k_1^+, k_2^+) Q_R^{(i)}(k_1^+, k_2^+) \phi_M(x) \right] \\ A_{00}^{(D2*)} &= \frac{N^{D_2^*} \epsilon^{*\sigma\nu} v_\sigma v_\nu}{4(\omega_0+1)(\omega_0-1)} \int_0^1 dx dz \int dk_1^+ dk_2^+ \left[C_L^{(i)}(z) J^{(i)}(z, x, k_1^+, k_2^+) Q_L^{(i)}(k_1^+, k_2^+) \phi_M(x) \right. \\ &\quad \left. + C_R^{(i)}(z) J^{(i)}(z, x, k_1^+, k_2^+) Q_R^{(i)}(k_1^+, k_2^+) \phi_M(x) \right]. \end{aligned} \quad (32)$$

Once again the vanishing of $C_R^{(0,8)}$ in Eq. (32) at leading order in $\alpha_s(Q)$ and using the polarization sums in Eq. (24) gives the unpolarized amplitude squared

$$\sum_{pol} |A_{00}^{(D_1, D_2*)}|^2 = \frac{1}{24} \left| N^{(D_1, D_2*)} \int_0^1 dx dz \int dk_1^+ dk_2^+ \left[C_L^{(i)}(z) J^{(i)}(z, x, k_1^+, k_2^+) \right. \right. \\ \left. \left. \times Q_L^{(i)}(k_1^+, k_2^+) \phi_M(x) \right] \right|^2. \quad (33)$$

Since $N^{D_1} = N^{D_2*}$, at leading order in Λ_{QCD}/m_Q we can make a prediction for the unpolarized branching ratios

$$\frac{Br(\bar{B}^0 \rightarrow D_2^{*0} M^0)}{Br(\bar{B}^0 \rightarrow D_1^0 M^0)} = 1, \quad (34)$$

which is one of the main results of this paper. Note that from the point of view of naive factorization, this result is quite unexpected since the tensor meson D_2^* cannot be produced by a V-A current.

B. Power Counting and Next to Leading Order Contributions

1. Color Allowed Modes

We see that as required by HQS, the unpolarized amplitude in Eq. (25) is proportional to $(\omega_0 - 1)$ which is expected to provide a suppression of this leading order result. However, it is also accompanied by a factor of $(\omega_0 + 1)^2$. At maximum recoil ω_0 is related to the energy of the light meson and the mass of the charmed meson through

$$\sqrt{(\omega_0 + 1)(\omega_0 - 1)} = \frac{E_M}{m_D}. \quad (35)$$

Thus, in the SCET power counting scheme the quantity $\sqrt{(\omega_0 + 1)(\omega_0 - 1)}$ is of order one. It is now clear from Eq. (25) and the above relation that despite the constraint of HQS there is no suppression of the leading order result and the subleading corrections of order Λ_{QCD}/Q are not dangerous to the leading order result. This allows us to rely on the leading order predictions up to corrections suppressed by Λ_{QCD}/Q .

To illustrate the above ideas, in this section we will compute some of the subleading corrections and compare their sizes relative to the leading order predictions. The leading order operators in Eqs. (10) and (15) are products of soft and collinear operators $O = O_s * O_c$. Subleading corrections can arise in four possible ways

- corrections in the soft sector to O_s and from T-products (see Fig. 5a) with O_s .
- corrections in the collinear sector to O_c and from T-products (see for example Fig. 5b) with O_c .
- corrections from subleading mixed collinear-soft operators and their T-products.
- Beyond the heavy quark limit, s_l is no longer a good quantum number. From table I, we see that it implies mixing between D_1 and D_1^* . Thus, the physical D_1 state will have a small admixture of the D_1^* state beyond the heavy quark limit which will play a role in subleading corrections.

We will only focus on subleading corrections in the soft sector from HQET as in Fig. 5a in order to illustrate the power counting. These corrections give precisely the subleading semileptonic form factors which were computed in Ref. [21]. The analysis for the remaining subleading corrections will follow in a similar manner and we leave it as possible future work.

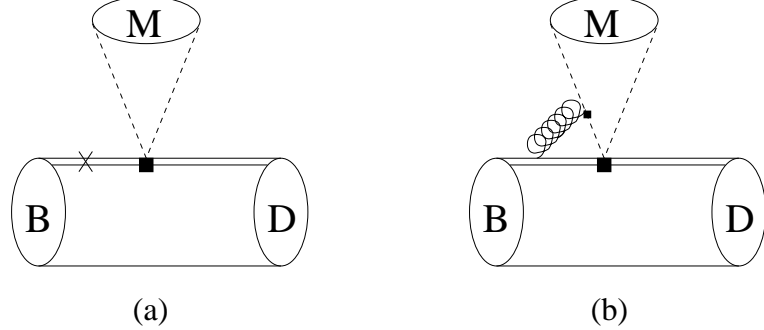


FIG. 5: Contributions to the color allowed sector from T-ordered products of the effective weak vertex in SCET_I with subleading kinetic and chromomagnetic HQET operators (a) and with the subleading SCET operators(b). In this section, to illustrate through examples the relative suppression the subleading contributions by at least Λ_{QCD}/Q , we only consider T-ordered products of type (a). The analysis for type (b) contributions will proceed in a similar manner.

The HQET and QCD fields are related to each other through

$$Q(x) = e^{-im_Q v \cdot x} [1 + \frac{i\vec{D}}{2m_Q} + \dots] h_v^{(Q)}, \quad (36)$$

where the ellipses denote terms suppressed by higher orders of Λ_{QCD}/m_Q and $Q = b, c$. Including the Λ_{QCD}/m_Q corrections, the QCD current is now matched onto

$$\bar{c}\Gamma b \rightarrow \bar{h}_{v'}^{(c)} (\Gamma - \frac{i}{2m_c} \vec{D}\Gamma + \frac{i}{2m_b} \Gamma \vec{D}) h_v^{(b)}. \quad (37)$$

Then there are subleading corrections from T-ordered products of the leading order current with order Λ_{QCD}/Q terms in the HQET Lagrangian:

$$\delta L_{HQET} = \frac{1}{2m_Q} [O_{kin,v}^{(Q)} + O_{mag,v}^{(Q)}] \quad (38)$$

where $O_{kin,v}^{(Q)}$ and $O_{mag,v}^{(Q)}$ are the kinetic and chromomagnetic operators

$$O_{kin,v}^{(Q)} = \bar{h}_v^{(Q)} (iD)^2 h_v^{(Q)}, \quad O_{mag,v}^{(Q)} = \bar{h}_v^{(Q)} \frac{g_s}{2} \sigma_{\alpha\beta} G^{\alpha\beta} h_v^{(Q)}. \quad (39)$$

We employ the trace formalism to compute these subleading corrections to the soft matrix element from corrections to the matching in Eq. (37)

$$\begin{aligned} \bar{h}_{v'}^{(c)} i \vec{D}_\lambda \gamma^\lambda \Gamma h_v^{(b)} &= Tr[S_{\sigma\lambda}^{(c)} \bar{F}_{v'}^{\sigma(c)} \gamma^\lambda \Gamma H_v^{(b)}] \\ \bar{h}_{v'}^{(c)} \Gamma \gamma^\lambda i \vec{D}_\lambda h_v^{(b)} &= Tr[S_{\sigma\lambda}^{(b)} \bar{F}_{v'}^{\sigma(c)} \Gamma \gamma^\lambda H_v^{(b)}], \end{aligned} \quad (40)$$

and from T-ordered products with δL_{HQET}

$$\begin{aligned} i \int d^4x T(O_{mag,v'}^{(c)}(x) [\bar{h}_{v'}^{(c)} \Gamma h_v^{(b)}](0)) &= Tr[R_{\sigma\alpha\beta}^{(c)} \bar{F}_{v'}^{\sigma(c)} i\sigma^{\alpha\beta} \frac{1+\not{p}}{2} \Gamma H_v^{(b)}] \\ i \int d^4x T(O_{mag,v}^{(b)}(x) [\bar{h}_{v'}^{(c)} \Gamma h_v^{(b)}](0)) &= Tr[R_{\sigma\alpha\beta}^{(b)} \bar{F}_{v'}^{\sigma(c)} \Gamma \frac{1+\not{p}}{2} i\sigma^{\alpha\beta} H_v^{(b)}] \end{aligned} \quad (41)$$

where the structures $S_{\sigma\lambda}^{(Q)}$ and $R^{(Q)}$ are parametrized as

$$\begin{aligned} S_{\sigma\lambda}^{(Q)} &= v_\sigma [\tau_1^{(Q)} v_\lambda + \tau_2^{(Q)} v'_\lambda + \tau_3^{(Q)} \gamma_\lambda] + \tau_4^{(Q)} g_{\sigma\lambda} \\ R_{\sigma\alpha\beta}^{(c)} &= n_1^{(c)} v_\sigma \gamma_\alpha \gamma_\beta + n_2^{(c)} v_\sigma v_\alpha \gamma_\beta + n_3^{(c)} g_{\sigma\alpha} v_\beta, \\ R_{\sigma\alpha\beta}^{(b)} &= n_1^{(b)} v_\sigma \gamma_\alpha \gamma_\beta + n_2^{(b)} v_\sigma v'_\alpha \gamma_\beta + n_3^{(b)} g_{\sigma\alpha} v'_\beta. \end{aligned} \quad (42)$$

The T-ordered products with the kinetic energy operator $O_{kin,v}^{(Q)}$ do not violate spin symmetry and simply provide Λ_{QCD}/m_Q corrections to the form factor in Eq. (19) $\tau \rightarrow \tilde{\tau} = \tau + \frac{\eta_{ke}^c}{2m_c} + \frac{\eta_{ke}^b}{2m_b}$. The form factors appearing in $S_{\sigma\lambda}^{(Q)}$ are not all independent and are related [21] through

$$\begin{aligned} \omega \tau_1^{(c)} + \tau_2^{(c)} - \tau_3^{(c)} &= 0 \\ \tau_1^{(b)} + \omega \tau_2^{(b)} - \tau_3^{(b)} + \tau_4^{(b)} &= 0 \\ \tau_1^{(c)} + \tau_1^{(b)} &= \bar{\Lambda} \tau \\ \tau_2^{(c)} + \tau_2^{(b)} &= -\bar{\Lambda}' \tau \\ \tau_3^{(c)} + \tau_3^{(b)} &= 0 \\ \tau_4^{(c)} + \tau_4^{(b)} &= 0, \end{aligned} \quad (43)$$

where $\bar{\Lambda}$ and $\bar{\Lambda}'$ are the energies of the light degrees of freedom in the $m_{b,c} \rightarrow \infty$ limit for the (\bar{B}, \bar{B}^*) and (D_1, D_2^*) HQS doublets respectively. Using these relations we can express our results in terms of the τ , $\tau_1^{(c)}$, and $\tau_2^{(c)}$ form factors. Combining the subleading contributions from Eqs. (40) and (41) with the leading order result in Eq. (19) and using constraints from Eq. (43) we can write the soft matrix element as

$$\begin{aligned} S_{D1,D2*} &= \tilde{\tau}(\omega_0) \text{Tr} [v_\sigma \bar{F}_{v'}^{(c)\sigma} \Gamma H_v^{(b)}] - \frac{1}{2m_c} \text{Tr}[S_{\sigma\lambda}^{(c)} \bar{F}_{v'}^{\sigma(c)} \gamma^\lambda \Gamma H_v^{(b)}] - \frac{1}{2m_b} \text{Tr}[S_{\sigma\lambda}^{(c)} \bar{F}_{v'}^{\sigma(c)} \Gamma \gamma^\lambda H_v^{(b)}] \\ &+ \frac{\tau(\omega)}{2m_b} \text{Tr}[(\bar{\Lambda} v_\lambda - \bar{\Lambda}' v'_\lambda) v_\sigma \bar{F}_{v'}^{\sigma(c)} \Gamma \gamma^\lambda H_v^{(b)}] + \frac{1}{2m_c} \text{Tr}[R_{\sigma\alpha\beta}^{(c)} \bar{F}_{v'}^{\sigma(c)} i\sigma^{\alpha\beta} \frac{1+\not{p}}{2} \Gamma H_v^{(b)}] \\ &+ \frac{1}{2m_b} \text{Tr}[R_{\sigma\alpha\beta}^{(b)} \bar{F}_{v'}^{\sigma(c)} \Gamma \frac{1+\not{p}}{2} i\sigma^{\alpha\beta} H_v^{(b)}] + \dots, \end{aligned} \quad (44)$$

where the ellipses denote contributions from other subleading operators that we have not considered. Computing the above traces and combining the results for the hard and collinear parts from section II, the amplitudes can be brought into the final form

$$\begin{aligned} A(B \rightarrow D_1 M) &= N^{D1} f^{BD1} \epsilon^* \cdot v \int_0^1 dx T^{D1}(x, m_c/m_b, \mu) \phi_M(x, \mu) \\ A(B \rightarrow D_2^* M) &= N^{D2*} f^{BD2*} \epsilon^{*\sigma\nu} v_\sigma v_\nu \int_0^1 dx T^{D2*}(x, m_c/m_b, \mu) \phi_M(x, \mu), \end{aligned} \quad (45)$$

where $f^{(BD1, BD2*)}$ are functions of the form factors $\tilde{\tau}, \tau_1^{(c)}, \tau_2^{(c)}, \eta_{1,2,3}^{(c,b)}$. For the D_1 channel, f^{BD1} is given by

$$\begin{aligned} \sum_{pol} |\epsilon^* \cdot v \bar{f}^{BD1}|^2 &= \frac{m_B(\omega_0 + 1)}{12m_D} \\ &\times \left[\left(2\tilde{\tau} + \frac{6\eta_1^{(c)}}{m_c} - \frac{2\eta_2^{(c)}}{m_c} - \frac{\eta_3^{(c)}}{m_c} + \frac{6\eta_1^{(b)}}{m_b} + \frac{\eta_2^{(b)}}{m_b} + \frac{\eta_3^{(b)}}{m_b} \right. \right. \\ &+ \left(\frac{m_B}{m_D} + \frac{m_D}{m_B} \right) \frac{\eta_2^{(c)}}{m_c} - \left(\frac{m_B}{m_D} + \frac{m_D}{m_B} - 1 \right) \frac{\eta_2^{(b)}}{m_b} \Big) \sqrt{(\omega_0 + 1)(\omega_0 - 1)} \quad (46) \\ &- \left(\frac{m_B^2}{m_D^2} + \frac{m_D^2}{m_B^2} \right) \frac{\tau_1^{(c)}}{2m_c} + \left(\frac{\tau_2^{(c)}}{m_c} - \frac{2\bar{\Lambda}\tau}{m_c} \right) + \left(\frac{m_B}{m_D} + \frac{m_D}{m_B} \right) \left(\frac{\bar{\Lambda}'\tau}{m_c} + \frac{\tau_1^{(c)}}{2m_c} - \frac{\tau_2^{(c)}}{2m_c} \right) \\ &\left. \left. + \left(\frac{m_B}{m_D} + \frac{m_D}{m_B} + 1 \right) \frac{\tau_1^{(c)}}{m_b} \sqrt{(\omega_0 - 1)} + \left(\frac{\tau_2^{(c)}}{m_b} - \frac{\bar{\Lambda}\tau}{m_b} - \frac{\bar{\Lambda}'\tau}{m_b} \right) (\omega_0 - 1) + \dots \right)^2, \right. \end{aligned}$$

and for the D_2 channel, f^{BD2} is given by

$$\begin{aligned} \sum_{pol} |\epsilon^{*\sigma\nu} v_\sigma v_\nu \bar{f}^{BD2*}|^2 &= \frac{m_B(\omega_0 + 1)}{12m_D} \\ &\times \left[\left(2\tilde{\tau} - \frac{2\eta_1^{(c)}}{m_c} + \frac{\eta_2^{(c)}}{m_c} + \frac{\eta_3^{(c)}}{m_c} - \frac{\tau_2^{(c)}}{m_c} + \frac{6\eta_1^{(b)}}{m_b} + \frac{\eta_2^{(b)}}{m_b} + \frac{\eta_3^{(b)}}{m_b} \right. \right. \\ &+ \left(\frac{m_B}{m_D} + \frac{m_D}{m_B} - 1 \right) \left(\frac{\tau_1^{(c)}}{m_c} - \frac{\eta_2^{(b)}}{m_b} \right) \Big) \sqrt{(\omega_0 + 1)(\omega_0 - 1)} \quad (47) \\ &- \left. \left. \left((\bar{\Lambda} + \bar{\Lambda}') \frac{\tau}{m_b} - \frac{\tau_2^{(c)}}{m_b} - \left(\frac{m_B}{m_D} + \frac{m_D}{m_B} + 1 \right) \left(\frac{\eta_2^{(c)}}{m_c} - \frac{\tau_1^{(c)}}{m_b} \right) \right) (\omega_0 - 1) + \dots \right)^2. \right. \end{aligned}$$

The above expressions are written in a way to make the power counting manifest. The ratio $\frac{m_B}{m_D}$ is of order one, $(\omega_0 - 1)$ is numerically of order Λ_{QCD}/Q , and as discussed in Eq. (35) the quantity $\sqrt{(\omega_0 - 1)(\omega_0 + 1)}$ is of order one. We see that the leading order contribution inside the square brackets in Eqs. (46) and (47) is proportional to $\tau \sqrt{(\omega_0 - 1)(\omega_0 + 1)}$ and is the same for the D_1 and D_2^* channels. More importantly, there is no suppression of the leading order term due to HQS since $\sqrt{(\omega_0 - 1)(\omega_0 + 1)}$ is of order one. On the other hand, the subleading corrections in the square brackets are of size either Λ_{QCD}/m_Q , $(\omega_0 - 1)\Lambda_{QCD}/m_Q$, $\sqrt{(\omega_0 - 1)\Lambda_{QCD}/m_Q}$, or $\sqrt{(\omega_0 - 1)(\omega_0 + 1)\Lambda_{QCD}/m_Q}$ and hence are suppressed by at least Λ_{QCD}/m_Q relative to the leading order prediction. Thus, we see that the constraints of HQS enter in a very specific manner so as to preserve the power counting scheme of SCET allowing us to ignore the subleading corrections near maximum recoil. It was the maximum recoil relation in Eq. (35) that ensured no suppression of the leading order result. The predictions of Eq. (26) remain intact with these subleading corrections suppressed by at least Λ_{QCD}/Q .

2. Color Suppressed Modes

In the case of color suppressed decays which are mediated by operators that are not conserved currents, there is no reason to expect the soft matrix element to vanish at zero

recoil by HQS and thus no reason to expect a suppression at maximum recoil. In fact the non-trivial dependence of the soft matrix elements in Eq. (27) on the light cone vector n_μ makes it difficult to make a comparison with the zero recoil limit. The soft functions $Q_{L,R}^{(0,8)}$ will depend on the light cone vector n^μ through the arguments $(n \cdot v, n \cdot v', n \cdot k_1, n \cdot k_2)$ and it is not obvious how to extrapolate such a function away from maximum recoil. At maximum recoil v, v' and n are related through

$$m_B v^\mu = m_D v'^\mu + E_M n^\mu. \quad (48)$$

The light cone vector has the special property $n^2 = 0$ and is a reflection of the onshell condition of the pion $p_\pi^2 = (E_\pi n)^2 = 0$. Away from maximum recoil, $E_M n^\mu$ is to be replaced by q^μ which is offshell $q^2 \neq 0$, inconsistent with the $n^2 = 0$ property of the light cone vector. So, Eq. (48) can no longer be used to determine n^μ in terms of v^μ and v'^μ and thus more care is required in extrapolating away from maximum recoil.

From Eqs. (32), (30), and (35) and the power counting scheme discussed earlier we see that there is in fact no suppression of the leading order color suppressed amplitude. The leading order predictions of Eq. (34) remain intact with corrections suppressed by at least Λ_{QCD}/Q . We leave the analysis of subleading corrections in the color suppressed sector as possible future work.

IV. PHENOMENOLOGICAL PREDICTIONS

In the color allowed sector, based on an analysis of semileptonic decays and an expansion in powers of $(\omega_0 - 1)$, the ratio in Eq. (26) was previously predicted to be in the range $0.1 - 1.3$ in Ref. [21] and 0.35 in Ref. [41]. In this paper, with the new power counting introduced at maximum recoil, we have shown the ratio to be one at leading order. In fact we have obtained the same result even for the color suppressed channel. The main results of this paper at leading order are the equality of branching fractions and strong phases

$$\frac{Br(\bar{B} \rightarrow D_2^* M)}{Br(\bar{B} \rightarrow D_1 M)} = 1, \quad \phi^{D_2^* M} = \phi^{D_1 M}, \quad (49)$$

where $M = \pi, \rho, K, K^*$ in the color allowed channel and $M = \pi, \rho, K, K_{||}^*$ in the color suppressed channel. This result in the color suppressed channel is quite unexpected from the point of view of naive factorization. In the color suppressed channel the long distance operators in Fig. 4c,d give non-vanishing contributions for kaons at leading order in $\alpha_s(Q)$ unlike the case of $M = \pi, \rho$. However, based on the same arguments [19] given for the case of B -decays to ground state charmed mesons the long distance contributions to the color suppressed decays $\bar{B}^0 \rightarrow D_1^0 \bar{K}^0$ and $\bar{B}^0 \rightarrow D_2^{0*} \bar{K}^0$ are equal and the result still holds. For K^* 's the long distance contributions are equal only when they are longitudinally polarized.

Once data is available for the color suppressed channel we can construct isospin triangles analogous to Fig. (2). With A_{0-} chosen as real, the strong phase $\phi^{D^{**M}}$ generated by the color suppressed channel A_{00} through the soft functions $Q_{L,R}^{(0,8)}$ in Eq. (30), is identical for D_1 and D_2^* . The isospin angle δ which is related to ϕ through Eq. (3) is also the same for D_1 and D_2^* . Thus, at leading order we predict the isospin triangles for D_1 and D_2^* to identically overlap.

Recent data [29, 30] reports the ratio of branching fractions in the color allowed channel

$$\frac{Br(B^- \rightarrow D_2^{*0} \pi^-)}{Br(B^- \rightarrow D_1^0 \pi^-)} = 0.79 \pm 0.11. \quad (50)$$

The deviation of this ratio from one, which will cause the isospin triangles to no longer overlap, can be attributed to subleading effects. The subleading effects shown to be suppressed by Λ_{QCD}/Q are expected to give a 20% correction, enough to bring agreement with current data. Thus, our claim that subleading corrections are suppressed Λ_{QCD}/Q is in agreement with current data.

V. SUMMARY AND CONCLUSIONS

In this paper we have presented a model independent analysis of two body B -decays to an excited charmed meson (D_1, D_2^*) and a light meson $M = \pi, \rho, K$. The $b \rightarrow c$ flavor changing effective Hamiltonian was matched onto operators in the soft-collinear effective theory (SCET) through a series of matching and running steps. Factorization of the soft and collinear degrees of freedom was achieved in SCET allowing us to use the tools of heavy quark symmetry (HQS) in the soft sector. The combination of factorization with HQS lead to quantitative predictions relating the D_1 and D_2^* amplitudes at leading order in Λ_{QCD}/Q where $Q = \{m_b, m_c, E_M\}$.

The analysis closely paralleled the analysis for B -decays with ground state charmed mesons $\bar{B} \rightarrow D^{(*)} M$ [19]. At leading order, the results of factorization, generation of strong phases, and the Λ_{QCD}/Q suppression of color suppressed modes remain unchanged. Any differences show up only at the non-perturbative scale at which the binding of hadrons occurs. Thus, the Wilson coefficients that arise in matching calculations are identical and only the non-perturbative functions experience a change. Another difference unique to color allowed decays to excited charmed mesons arises from the constraint of HQS. The leading order amplitude is required to be proportional to $(\omega_0 - 1)$ which is numerically the same order as Λ_{QCD}/m_c . The study of semileptonic B -decays [21] near zero recoil suggests that the presence of powers of $(\omega_0 - 1)$ could suppress the leading order amplitude. However, in this paper we have shown that maximum recoil is a special kinematic point where the HQS constraints enter in a manner that preserves the SCET power counting scheme with no suppression from $(\omega_0 - 1)$. This was done by introducing a new power counting scheme for factors of $(\omega_0 - 1)$ unique to maximum recoil kinematics. We can safely rely on leading order predictions with corrections suppressed by at least one power of Λ_{QCD}/Q . This was explicitly verified for contributions from subleading semileptonic form factors.

At leading order we have shown the equality of the branching fractions $\bar{B} \rightarrow D_1 M$ and $\bar{B} \rightarrow D_2^* M$ and their strong phases. Once data on the color suppressed channels becomes available we can construct isospin triangles similar to those in Fig. 2. Other phenomenological predictions similar to the ones in section VI of [19] can be made can be made to leading order in $\alpha_s(\Lambda_{QCD}Q)$ by using tree level expressions for the jet functions J .

Possible future work includes computing the remaining subleading corrections to account for the 20% deviation of the data from the leading order predictions. The analysis could also be repeated for B -decays to other excited charmed mesons such as D_0^* and D_1^* .

Acknowledgments

I would like to thank I.W.Stewart for suggesting this problem and for the many discussions and comments on the manuscript. I would also like to thank Dan Pirjol for many useful comments and suggestions. This work is supported in part by funds provided by the U.S. Department of Energy (D.O.E) under the cooperative research agreement DF-FC02-94ER40818.

- [1] M. Bauer, B. Stech and M. Wirbel, *Z. Phys. C* **34**, 103 (1987).
- [2] M. J. Dugan and B. Grinstein, *Phys. Lett. B* **255**, 583 (1991).
- [3] M. Neubert and B. Stech, *Adv. Ser. Direct. High Energy Phys.* **15**, 294 (1998) [arXiv:hep-ph/9705292]; A. Ali, G. Kramer and C. D. Lu, *Phys. Rev. D* **58**, 094009 (1998) [arXiv:hep-ph/9804363]; H. Y. Cheng and B. Tseng, *Phys. Rev. D* **58**, 094005 (1998) [arXiv:hep-ph/9803457].
- [4] B. Blok and M. A. Shifman, *Nucl. Phys. B* **389**, 534 (1993) [arXiv:hep-ph/9205221]; I. E. Halperin, *Phys. Lett. B* **349**, 548 (1995) [arXiv:hep-ph/9411422].
- [5] A. J. Buras and L. Silvestrini, *Nucl. Phys. B* **569**, 3 (2000) [arXiv:hep-ph/9812392].
- [6] H. D. Politzer and M. B. Wise, *Phys. Lett. B* **257**, 399 (1991).
- [7] M. Beneke, G. Buchalla, M. Neubert and C. T. Sachrajda, *Nucl. Phys. B* **591**, 313 (2000) [arXiv:hep-ph/0006124].
- [8] Z. Ligeti, M. E. Luke and M. B. Wise, *Phys. Lett. B* **507**, 142 (2001) [arXiv:hep-ph/0103020].
- [9] C. W. Bauer, D. Pirjol and I. W. Stewart, *Phys. Rev. Lett.* **87**, 201806 (2001) [arXiv:hep-ph/0107002].
- [10] Z. z. Xing, arXiv:hep-ph/0107257.
- [11] M. Neubert and A. A. Petrov, *Phys. Lett. B* **519**, 50 (2001) [arXiv:hep-ph/0108103].
- [12] C. W. Bauer, B. Grinstein, D. Pirjol and I. W. Stewart, *Phys. Rev. D* **67**, 014010 (2003) [arXiv:hep-ph/0208034].
- [13] C. W. Chiang and J. L. Rosner, *Phys. Rev. D* **67**, 074013 (2003) [arXiv:hep-ph/0212274].
- [14] Z. z. Xing, *Eur. Phys. J. C* **28**, 63 (2003) [arXiv:hep-ph/0301024].
- [15] H. n. Li, arXiv:hep-ph/0303116.
- [16] C. W. Bauer, D. Pirjol, I. Z. Rothstein and I. W. Stewart, arXiv:hep-ph/0401188.
- [17] C. W. Bauer, S. Fleming and M. Luke, *Phys. Rev. D* **63**, 014006 (2001) [hep-ph/0005275]. C. W. Bauer, S. Fleming, D. Pirjol and I. W. Stewart, *Phys. Rev. D* **63**, 114020 (2001) [arXiv:hep-ph/0011336]. C. W. Bauer and I. W. Stewart, *Phys. Lett. B* **516**, 134 (2001) [arXiv:hep-ph/0107001].
- [18] C. W. Bauer, D. Pirjol and I. W. Stewart, *Phys. Rev. D* **65**, 054022 (2002) [arXiv:hep-ph/0109045].
- [19] S. Mantry, D. Pirjol and I. W. Stewart, *Phys. Rev. D* **68** (2003) 114009 [arXiv:hep-ph/0306254].
- [20] N. Sinha, arXiv:hep-ph/0405061.
- [21] A. K. Leibovich, Z. Ligeti, I. W. Stewart and M. B. Wise, *Phys. Rev. D* **57**, 308 (1998) [arXiv:hep-ph/9705467].
- [22] K. Hagiwara *et al.* [Particle Data Group Collaboration], *Phys. Rev. D* **66**, 010001 (2002).
- [23] A. Satpathy *et al.* [Belle Collaboration], *Phys. Lett. B* **553**, 159 (2003) [arXiv:hep-ex/0211022].

- [24] A. K. Leibovich, Z. Ligeti, I. W. Stewart and M. B. Wise, Phys. Lett. B **586** (2004) 337 [arXiv:hep-ph/0312319].
- [25] N. Isgur and M. B. Wise, Phys. Lett. B **232**, 113 (1989).
- [26] N. Isgur and M. B. Wise, Phys. Lett. B **237**, 527 (1990).
- [27] A. V. Manohar and M. B. Wise, Cambridge Monogr. Part. Phys. Nucl. Phys. Cosmol. **10**, 1 (2000).
- [28] S. Mantry, D. Pirjol and I. W. Stewart, arXiv:hep-ph/0401058.
- [29] K. Abe *et al.* [Belle Collaboration], arXiv:hep-ex/0307021.
- [30] B. Aubert *et al.* [BABAR Collaboration], arXiv:hep-ex/0308026.
- [31] N. Isgur and M. B. Wise, Phys. Rev. Lett. **66**, 1130 (1991).
- [32] T. Becher, R. J. Hill and M. Neubert, Phys. Rev. D **69**, 054017 (2004) [arXiv:hep-ph/0308122].
- [33] M. Beneke and T. Feldmann, Nucl. Phys. B **685**, 249 (2004) [arXiv:hep-ph/0311335].
- [34] C. W. Bauer, M. P. Dorsten and M. P. Salem, arXiv:hep-ph/0312302.
- [35] G. Buchalla, A. J. Buras and M. E. Lautenbacher, Rev. Mod. Phys. **68**, 1125 (1996) [arXiv:hep-ph/9512380].
- [36] C. W. Bauer, D. Pirjol and I. W. Stewart, arXiv:hep-ph/0211069; D. Pirjol and I. W. Stewart, arXiv:hep-ph/0211251.
- [37] M. Beneke, A. P. Chapovsky, M. Diehl and T. Feldmann, Nucl. Phys. B **643**, 431 (2002) [arXiv:hep-ph/0206152].
- [38] R. J. Hill and M. Neubert, arXiv:hep-ph/0211018.
- [39] A. F. Falk, H. Georgi, B. Grinstein and M. B. Wise, Nucl. Phys. B **343**, 1 (1990).
- [40] H. Y. Cheng, C. K. Chua and C. W. Hwang, Phys. Rev. D **69** (2004) 074025 [arXiv:hep-ph/0310359].
- [41] M. Neubert, Phys. Lett. B **418**, 173 (1998) [arXiv:hep-ph/9709327].